Journal of Nepal Geological Society, 1998, Vol. 18, pp. 169-183

Interseismic uplift and strain accumulation in Nepal Himalaya

Nipun Kapur and R.C. Agrawal
Department of Earthquake Engineering
University of Roorkee, Roorkee-247667, India

ABSTRACT

Savage (1983, 1995) and Thatcher and Rundle (1984) have postulated elastic half space and viscoelastic coupling models of strain accumulation and earthquake occurrences at the upper surface of the subducting lithospheric plate called detachment. These models infer the presence of a locked zone on the detachment during interseismic periods. The analysis based on interseismic uplift data of about two decades in Nepal Himalaya indicates absence of the postulated locked zone and instead suggests occurrence of thrust fault type (up dip) slip on the entire detachment (Jackson and Bilham, 1994). A question then arises as to whether the strains are accumulating at all in this region. Further, if strains are accumulating we may like to investigate the process responsible. The answer is provided by a plausible model visualising strain accumulation due to differential motion of the medium particles on the detachment and those above it. This relative down dip motion of the medium particles on the detachment may be occurring even if the subducting and the overriding plates are not fully coupled or locked. Sections with high coupling on the detachment would have accumulated larger strains compared to those with low coupling. A temporal decrease in up dip slip rate on the detachment, by virtue of increase in coupling or strain hardening, further represents interseismic accumulation of shear strains. On the other hand, a temporal increase in up dip slip rate, when activates unstable motion, may culminate into occurrence of a large earthquake. This model explains the observed elevation changes in the Himalaya and corresponding inference of up dip slip on the detachment. It also provides plausible justification to the occurrence of moderate and great earthquakes on a part of the detachment lying primarily below the Lesser-Higher Himalaya.

INTRODUCTION

The earlier analysis of interseismic elevation changes in Nepal Himalaya and certain other subduction zones suggest the occurrence of thrust fault type slip on the detachment (Lisowiski et al., 1988; Chander and Gahalaut, 1994; Jackson and Bilham, 1994; Savage, 1995). The proposed drag, viscoelastic coupling, elastic-, and modified elastic-half space models of plate subduction, however, infer that one or more segments of the plate interface remain locked during the interseismic periods (Thatcher and Rundle, 1984; Savage, 1983, 1995). The question then arises about how does one explain this discrepancy in the inferred direction of motion. Is this discrepancy caused by limitations, such as using homogeneous half space model? In the analyses by earlier workers or stick slip models, need certain modifications to explain the occurrence of interseismic thrust fault type slip on the detachment at these subduction zones. In this regard, it may be mentioned that the inferred motion on a fault can even reverse direction, if models with inhomogeneous mediums are used instead of homogeneous ones (Savage, 1987). Several other studies also highlight the significance of incorporating inhomogenities and topography into the domain on the simulated displacement distributions (Meertens and Wahr, 1986; Du et al., 1994). As for the latter aspect of modifying the proposed models, Savage (1995) has pointed out that the entire main thrust zone may not be locked during interseismic periods. The locking may occur only at certain patches of the main thrust zone on the detachment.

Moreover, the interseismic accumulation of strains in stick slip models is associated with the occurrence of down dip motion on the locked segment of the detachment (Yoshioka et al., 1993; Savage, 1983). On the other hand, it is not clear whether strains can accumulate with the occurrence of interseismic up dip (thrust fault type) slip on the detachment. However, Lisowiski et al. (1988) suggest that strains would not accumulate, if no segment of the detachment is locked, Jackson and Bilham (1994) associate the occurrence of interseismic thrust fault type slip to aseismic release of a part of the accumulated strains for Nepal Himalaya. In contrast to this, Chander and Gahalaut (1994) associate occurrence of interseismic thrust fault type slip on the Himalayan detachment to the accumulation of earthquake generating strains.

In order to bridge this gap between the proposed models of stick slip subduction and the inferred direction of interseismic motion on the detachment, we will reanalyse observed elevation changes in Nepal Himalaya. The analysis would be done to explore whether the inference of interseismic thrust fault type slip is correct, or it is the artifact of using simplified homogeneous half space models by earlier workers. The analysis is concluded with the proposition of a new hypothesis of strain accumulation when thrust fault type slip is occurring on the detachment during interseismic periods.

MATHEMATICAL DEVELOPMENT

The earlier analyses of the observed interseismic elevation changes, for evaluating displacement (up dip slip or down dip motion) rates on the Himalayan detachment uses elastic dislocation theory. Whereas, in stick slip subduction models no dislocation occurs on the main thrust zone of the detachment during interseismic periods. The dislocation theory by itself does not account for the locking at the detachment. For this purpose, the locking at the detachment is represented as superposition of steady state subduction and imposed normal slip at the plate convergence rate upon the main thrust zone (Savage, 1983). It is also argued that steady state subduction does not contribute to the uplift at the earth's surface. Hence, only normal slip is assumed to be responsible for deformation at the surface of the earth. A number of geodetic observations show certain amount of permanent vertical deformation after completion of one earthquake cycle (Thatcher, 1984; Matsu'ura and Sato, 1989). In addition to this permanent deformation, a steady uplift of marine terraces on a time scale of years has also been reported in the literature (Sato and Matsu'ura, 1993; Bilham et al., 1997). Thus, the validity of the argument regarding no contribution of steady state subduction on surface uplift in the real earth case is not warranted for. Hence it may not be suitable for analysing interseismic elevation changes. In view of these limitations, we use an alternative approach in the present study, which does not necessarily require superposition representation and no contribution of steady state subduction on uplift to be valid. Since we are interested in interpreting the observed interseismic ground elevation changes in terms of displacement rates on the plate boundary fault, the deformation of the wedge shaped medium on upper side of this fault is simulated using the pertinent boundary value problem (BVP) of elasticity theory (Shimazaki, 1974).

The boundary Γ of the 2-D wedge shaped domain used in the present analysis is divided into two segments Γ_1 and Γ_S (Fig. 1), which represent the surface of the earth and the subsurface boundary of the accretionary wedge, respectively. To study the displacement rates on the detachment only the boundary segment symbol Γ_S is further subdivided into subsections symbol Γ_{S1}, representing the detachment, and symbol Γ_{S2}, the remaining subsurface boundary. To account for the variation in the displacement rates along the detachment, we assume that it consist of 'n' segments with differing displacement rates. The surface displacements W_{ji} of node j can be expressed as linear combination of displacements at subsurface segments i's of Γ_{S1}. In this case, the residual of computed and observed surface displacement rates, $d_j \left(= \sum_i w_{ji}\alpha_i \right)$ and d_j^0 respectively, at the jth node is given as,

$$e_j = d_j^0 - \sum_{i=1} w_{ji}\, a_i, \quad j=1,2,\ldots\ldots\ldots m \qquad (1)$$

Here are the weights representing the slip rates on different segments of the detachment. It is assumed that homogeneous boundary condition is applied on Γ_{S2} and Finite Element Method (FEM) is used to calculate the unit responses (W_{ji}) for all the n-segments of Γ_{S1}.

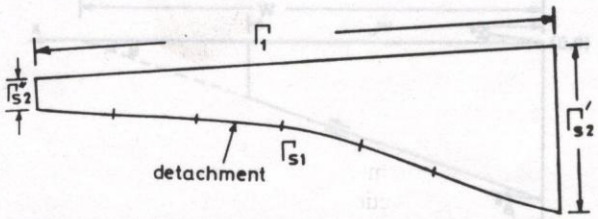

Fig. 1: The surface and subsurface segments Γ_1 and Γ_s of a 2-D wedge domain representing the cross-section of a mountain belt.

We pose our inverse problem as estimation of the set of α_i's which minimises the sum of squares of ε_j's over all j. The minimisation will be performed according to whether the unknown α_i's are constrained or not. Regarding the constraints on α_i's, as mentioned earlier, following two views exist in literature. In stick slip models, during interseismic period, the motion is constrained to occur in down dip direction on the main thrust zone. On the other hand, some of the have inferred the occurrence of up dip motion on the entire Nepal Himalayan detachment during the interseismic period. In order to evaluate these two view points, minimisation is carried out in the present study for three cases, when the displacements are constrained to occur in (i) down dip or (ii) up dip directions and (iii) when the direction of motion is not constrained at all. The corresponding inverted displacement rates are termed as type 1, type 2 and type 3 solutions.

It may be added here that if homogeneous boundary conditions are applied on Γ_{S2} then surface displacement rates are simply the effect of displacement rates on Γ_{S1}. To study the displacement rates on Γ_{S1} when those on Γ_{S2} are not zero (a more realistic situation), we solve the BVP with inhomogeneous Dirichlet boundary condition supplied on Γ_{S2}, while homogeneous Dirichlet and Neuman ones are supplied on Γ_1 and Γ_{S1}, respectively. The surface displacement rates due to this BVP are found out. These displacement rates are subtracted from the observed surface displacement rates to get the reduced observations. The reduced observations are purely due to the motion on subsurface boundary Γ_{S1}. To achieve this reduction we need to know the Dirichlet boundary condition on Γ_{S2}.

Boundary Conditions on Γ_{S2}

The insitu stress observations suggest linear variation of horizontal and vertical stresses with depth (Yin, 1993). This feature is utilized in designing the requisite displacement boundary condition. Theoretical stress expressions for a regular and homogeneous 2-D wedge model shown in Fig. 2 and derived elsewhere (Kapur, 1996) are used to find displacement distribution on the heel. These expressions are given as,

$$\begin{aligned}\sigma_x &= c_1x+c_2y \\ \sigma_y &= \rho gyCos\alpha \\ \tau_{xy} &= -c_1y-\rho gySin\alpha\end{aligned} \qquad (2)$$

Where, σ_x, σ_y are the normal stresses in x and y directions, τ_{xy} the shear stress, c_1, c_2 are the unknown constants, ρ is density of the medium, g is the acceleration due to gravity and α is the topographic slope. This kind of linear stress field have been used to model a number of mountain building characteristics and would be good enough as first approximation to find the boundary condition on Γ_{S2}. Towards translating these stress expressions to those of displacement, we use the following constraints on the displacement distribution:

The observations in an accretionary wedge show that the material gets accreted at the toe, buries within the wedge and gets uplifted at the rear (Platt, 1986; Dahlen and Barr, 1989). Thus the vertical velocity of rocks is zero at the front, while the horizontal velocity becomes zero at the rear of wedge. Therefore,

$$\begin{aligned}&\text{(i) } u = 0 \quad \text{at } x = 0,\ y = 0 \\ &\text{(ii) } v = 0 \quad \text{at } x = w_o,\ y = 0\end{aligned} \qquad (3)$$

where wo is length of the wedge (Fig. 2).

Here, u and v are the displacements occurring in x and y directions in one year.

Using the constraints given by expressions (3) and neglecting the effect of gravity we get the following general displacement expressions:

$$u = \frac{1}{E}\left[\frac{c_1x^2}{2} + c_2xy\right] - \frac{(2+v)}{2E}c_1y \qquad (4)$$

$$v = \frac{1}{E}\left[-v(c_1xy+c_2)\right] - \frac{c_2x^2}{2E} + \frac{c_2 w_0^2}{2E}$$

To find the unknowns c_1 and c_2 following constraints on displacement distribution are used:

(i) $v = V_{obs}\text{Cos}\alpha$ (5)

(ii) $u\text{Sin}\theta + v\text{Cos}\theta = 0$ on $y = (W-x)\tan\theta$ for $x = 0$

Here W is the total length of the wedge from the sharp taper as shown in the Fig. 2.

In the first of these displacement constraints, the y-component of the observed change in elevation, $V_{obs}\text{Cos}\alpha$, at some point on the surface of the wedge is used to find the unknown c_2. While in the second boundary condition, we take that no fault normal displacements occurs on the base (detachment) of the wedge. Applying these two conditions equation (4) gives,

$$c_2 = \frac{2EV_{obs}\text{Cos}\alpha}{w_0^2 - x'^2} \quad (6)$$

and

$$c_1 = \frac{c_2\,(w_0^2 - v\text{Wtan}\theta)}{\text{Wtan}^2\theta\,\tan\alpha\,(2+v)} \quad (7)$$

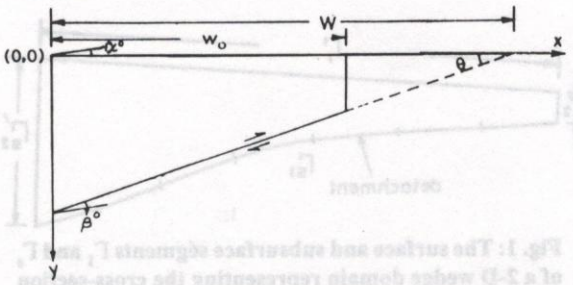

Fig. 2: Wedge model used to derive stress expressions (2).

INTERSEISMIC OBSERVATIONS IN NEPAL HIMALAYA

The repeated levelling line, used to study the displacement rates on the detachment, runs from Birganj in the Indo-Gangetic plains to Kodari just to the north of the Main Central Thrust (MCT). The total length of this line is about 350 km (Fig. 3). The length of profile perpendicular to the Himalayan strike is about 132 km. The data are taken from Jackson and Bilham (1994). The measurements were made twice between 1977 and 1990, i.e. later to the 1934 great earthquake and hence represent the interseismic geodetic data. Eventhough no large earthquakes have

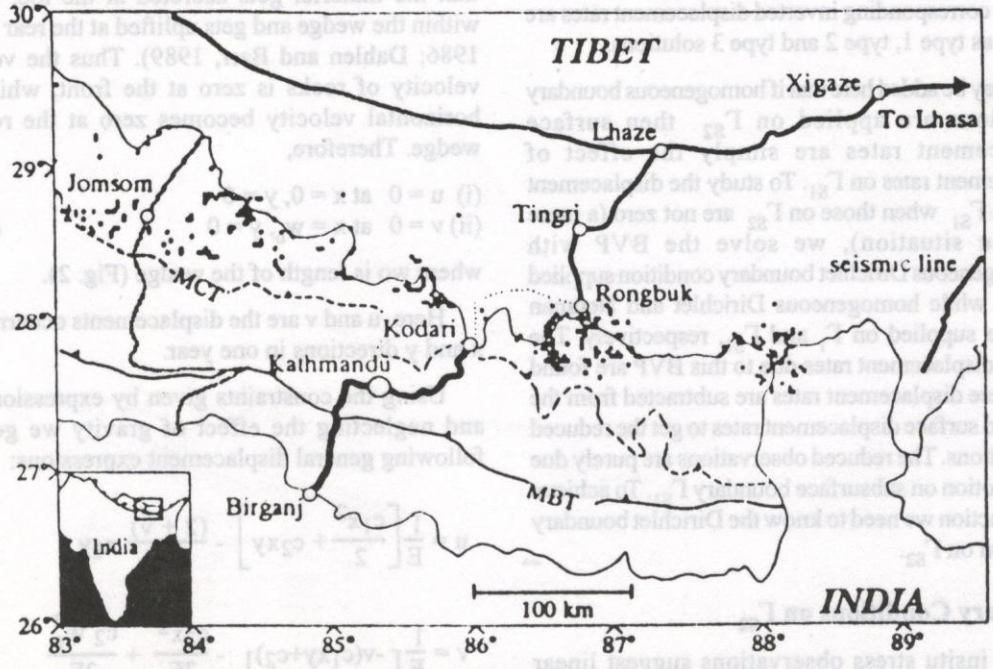

Fig. 3: Location of levelling line in Nepal Himalaya (after Jackson and Bilham, 1994).

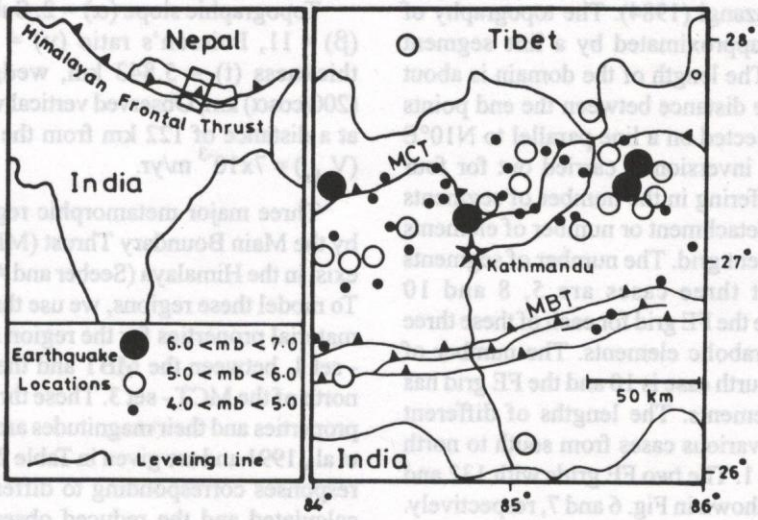

Fig. 4: Location of levelling line and epicentres of earthquakes recorded in the vicinity during 1911 to 1990. No large events have been recorded during the period 1975 to 1990 in the region (after Jackson et al., 1992). Legend: MCT - Main Central Thrust, MBT - Main Boundary Thrust.

occurred during 1975 to 1990, yet a number of events (including large) have been recorded during the period 1911 to 1975 in the region (Fig. 4) thereby suggesting presence and release of strains as earthquakes. The elevation changes per year and the random errors with respect to Birganj are shown in Fig. 5. The random errors in the observations is give by $1.1\sqrt{L}$ mm, where L is the along line length in kilometers. On the other hand, systematic errors can exceed 1 cm per vertical kilometer. The along line random errors in the uplift rate data can grow to 7 mm/yr from the plains of India to Tibet. In addition, a systematic error of about 3 3 mm/yr may also exist.

ANALYSIS OF INTERSEISMIC ELEVATION CHANGES

The wedge shaped domain used for inversion represents a cross-section of Nepal Himalaya taken

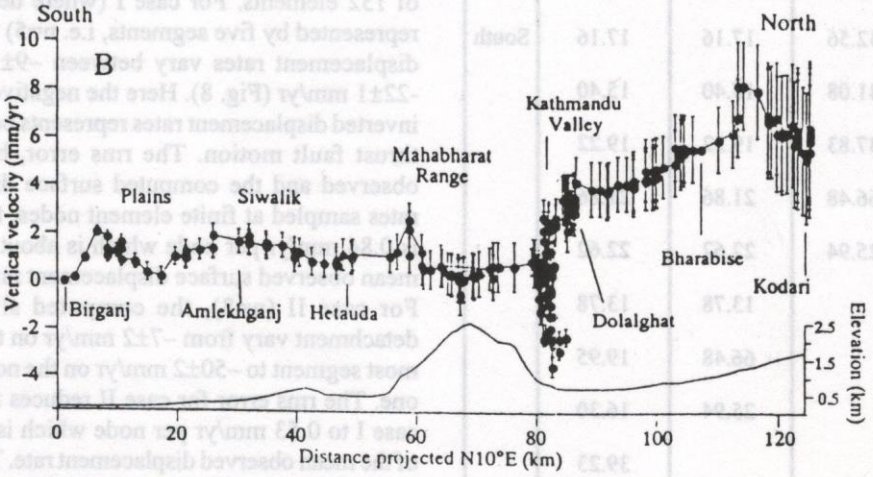

Fig. 5: The elevation changes per year and the random errors with respect to the bench mark at Birganj (after Jackson and Bilham, 1994).

from Ni and Barazangi (1984). The topography of the Himalaya is approximated by a line segment having 2 slopes. The length of the domain is about 200 km, while the distance between the end points of the profile projected on a line parallel to N10°E is 122 km. In all inversion is carried out for four cases (I to IV) differing in the number of segments representing the detachment or number of elements in the Finite Element grid. The number of segments used in the first three cases are 5, 8 and 10 respectively, while the FE grid for each of these three cases has 132 parabolic elements. The number of segments in the fourth case is 10 and the FE grid has 173 parabolic elements. The lengths of different segments S_i's for various cases from south to north are given in Table 1. The two FE grids with 132 and 173 elements are shown in Fig. 6 and 7, respectively.

The observations are first reduced before inversion. To effect the reduction of the observed elevation change data in Nepal Himalaya, the magnitude of various parameters (Fig. 2) used to calculate displacement rates on rear vertical boundary of the wedge are:

Table 1: Length of different segments from south to north used together to represent Nepal Himalayan detachment in the present study.

Segment	Length for different cases (km)			
	5 segments	8 segments	10 segments	
S1	32.56	17.16	17.16	South
S2	41.08	15.40	15.40	
S3	37.83	19.22	19.22	
S4	66.48	21.86	21.86	
S5	25.94	22.62	22.62	
S6		13.78	13.78	
S7		66.48	19.95	
S8		25.94	16.30	
S9			39.23	
S10			25.94	North

Topographic slope (α) = 2, Subducting plate dip (β) = 11, Poisson's ratio (ν) = 0.26, wedge toe thickness (t) = 5.843 km, wedge length (w_o) = (200/cosα) km, Observed vertical velocity on surface at a distance of 122 km from the toe of the wedge (V_{obs}) = 7×10^{-3} m/yr.

Three major metamorphic regions, demarcated by the Main Boundary Thrust (MBT) and the MCT, exist in the Himalaya (Seeber and Armbruster, 1981). To model these regions, we use three distinct sets of material properties for the region south of the MBT - set 1, between the MBT and the MCT -set 2, and north of the MCT - set 3. These three sets of material properties and their magnitudes are taken from Singh et al., 1991 and are given in Table 2. The unit impulse responses corresponding to different segments are calculated and the reduced observations inverted. The inverted displacement rates are given in Table 3. The observed and the computed surface displacement rates for the solutions with lowest rms difference (errors) together with the slip rates on different segments of the detachment are plotted in Fig. 8 to 11.

RESULTS AND DISCUSSION

Absence of Interseismic Locked Zone

We will first present the inverted displacement rates on the detachment, when these are unconstrained (type 1 solution) and FE- grid consists of 132 elements. For case I (where detachment is represented by five segments, i.e. n=5) the inverted displacement rates vary between –9±1 mm/yr to -22±1 mm/yr (Fig. 8). Here the negative sign in the inverted displacement rates represents occurrence of thrust fault motion. The rms error, between the observed and the computed surface displacement rates sampled at finite element nodes, for this case is 0.84 mm/yr per node which is about 33% of the mean observed surface displacement rate (Table 3). For case II (n=8), the computed slip rates on detachment vary from –7±2 mm/yr on the southern most segment to –50±2 mm/yr on the northern most one. The rms error for case II reduces from that of case I to 0.53 mm/yr per node which is about 21% of the mean observed displacement rate. The inverted displacement rates for case III (n=10) vary between –7±2 mm/yr to -46.5±2 mm/yr, while the rms error

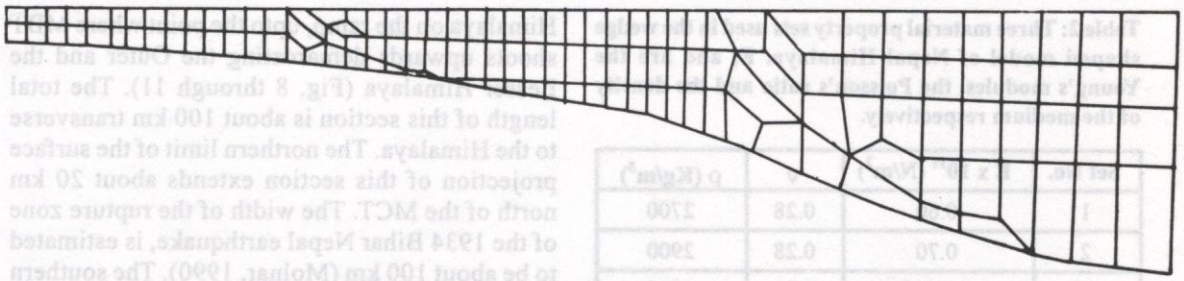

Fig. 6: The domain and the 132 element FE grid laid to analyse the Nepal Geodetic data.

is same as that of case II. For the 173 element FE grid, the slip rates vary between –8±3 mm/yr to -50±3 mm/yr. The rms error in this case increases (from that of case II and III) to 0.55 mm/yr per node which is about 22% of the mean observed displacement rate. For the various cases mentioned above, the slip rate on different segments below the Lesser and Higher Himalaya, except for the northernmost, lies between –9±2 mm/yr to –30±3 mm/yr and hence are in accordance with the earlier proposed convergence rates of 18±7 mm/yr (Molnar and Lyon Caen, 1989) and 20±10 mm/yr (Armijo et al., 1986). The differences in solutions when the motion on the detachment is unconstrained and constrained to occur in updip direction (type 1 and type 2 solutions respectively) are small except for the two northernmost segments (Table 3). For these northernmost segments the difference reaches upto 40 mm/yr. The rms errors for type 3 solutions, where motion on the detachment is constrained to occur in normal fault sense, are about 450 % larger than those of type 1 and type 2 solutions and for different cases have magnitudes greater than or equal to the mean observed displacement rates (Table 3). It has been mentioned above that the inverted slip rates on the northernmost segment show oscillations for the different cases I through IV. Its value for type 1 solutions vary from –6±3 mm/yr to –50±2 mm/yr (Table 3). One of the explanations for this large variation is the lack of observational data to the north of the MCT. In other words, no good control of slip on the heelward segments is possible from the available surface data.

The inverted displacement rates on the detachment and the degree of match between the observed and the computed surface displacement rates (Table 3) shows that thrust fault type rather than normal fault type motion, is more likely to be occurring even during the interseismic period. The occurrence of thrust fault motion has also been inferred by the earlier workers (Jackson and Bilham, 1994; Chander and Gahalaut, 1994) and supports the result of the present study.

Variable Coupling Along the Himalayan Detachment

On the basis of physical evidences, a section of high coupling bounded in front and rear by portions of low coupling is treated as characteristic of plate interface (Yoshioka et al., 1993; Hyndman and Wang, 1993; Pacheco et al., 1993). In the present study, we were able to identify regions of low-high-low coupling along

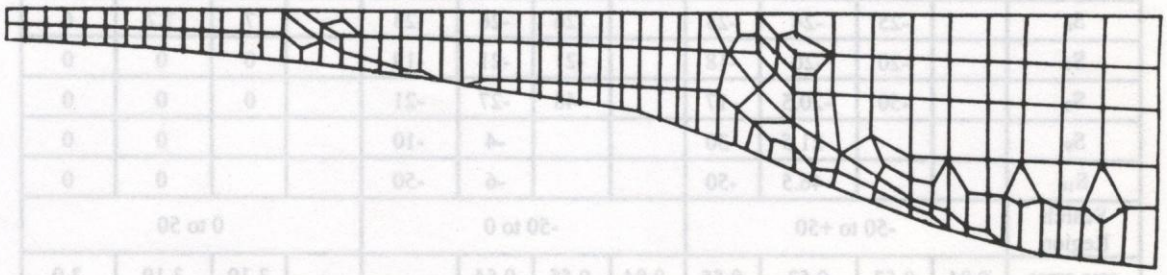

Fig. 7: The domain and the 173 element FE grid used to analyse Nepal Geodetic data.

Table 2: Three material property sets used in the wedge shaped model of Nepal Himalaya. E, and are the Young's modules, the Poisson's ratio and the density of the medium respectively.

Set No.	E x 10^{11} (N/m^2)	ν	ρ (Kg/m^3)
1	0.60	0.28	2700
2	0.70	0.28	2900
3	0.65	0.25	2700

the detachment. The section of high coupling, on the detachment primarily exist underneath Nepal Lesser Himalaya and is made up of two nearly contiguous portions of low updip slip rate than on the adjoining segments (Fig. 8 through 11). These two portions about 23 km and about 67 km long have slip rates of 10 mm/yr and 20 mm/yr respectively. The intervening segment is about 14 km long and has a slip rate of 25 mm/yr. The inverted results of the Nepal profile show that the region of high coupling on the detachment extend roughly from a point below the Greater Himalaya on the ramp, upto the point where MBT shoots upwards demarcating the Outer and the Lesser Himalaya (Fig. 8 through 11). The total length of this section is about 100 km transverse to the Himalaya. The northern limit of the surface projection of this section extends about 20 km north of the MCT. The width of the rupture zone of the 1934 Bihar Nepal earthquake, is estimated to be about 100 km (Molnar, 1990). The southern and northern limits of this rupture zone is proposed to lie below the southern margin of the Lesser and Higher Himalaya, respectively (Chander, 1989; Molnar and Pandey, 1989). Thus, the inferred section of low thrust fault type slip rate (high coupling) coincides well with the proposed rupture zone during the 1934 great earthquake. Fig. 4 shows the occurrence of small and moderate magnitude earthquakes from 1911 to 1990 close to the leveling line (Jackson et al., 1992). Further, Pandey et al. (1995) show occurrence of intense microseismicity close to the Himalayan ramp. Hence, the identified region of

Table 3: Inverted displacement rates on different segments of the detachment, search region (mm/yr) in solution space, rms errors (mm yr^{-1}/node) between the observed and the computed surface uplift rates, and the uncertainty (mm/yr) in the inverted slip rates for different cases and different types of motion.

Segment	Type 1				Type 2				Type 3			
	Case I	Case II	Case III	Case IV	Case I	Case II	Case III	Case IV	Case I	Case II	Case III	Case IV
S_1	-9	-7	-7	-8	-9	-7	-7	-6	7	5	5.2	6
S_2	-15	-10	-11	-10	-15	-10	-12	-11	5.1	6	5.5	6
S_3	-13	-14	-15	-16	-13	-14	-16	-14	7.2	3	3	3
S_4	-19	-14	-15	-16	-19	-14	-16	-14	0	6	5.5	6
S_5	-22	-9	-11	-10	-26	-10	-10	-10	0	7	7.2	6
S_6		-25	-24	-25		-26	-26	-23		7	7.2	6
S_7		-20	-20	-18		-21	-21	-19		0	0	0
S_8		-50	-20.5	-17		-48	-27	-21		0	0	0
S_9			-21.5	-30			-4	-10			0	0
S_{10}			-46.5	-50			-6	-50			0	0
Search Region	-50 to +50				-50 to 0				0 to 50			
rms error	0.84	0.53	0.53	0.55	0.84	0.55	0.54	-	-	3.19	3.19	3.0
Uncertainty	1	2	2	3	1	2	3	-	0.1	1	1.2	3

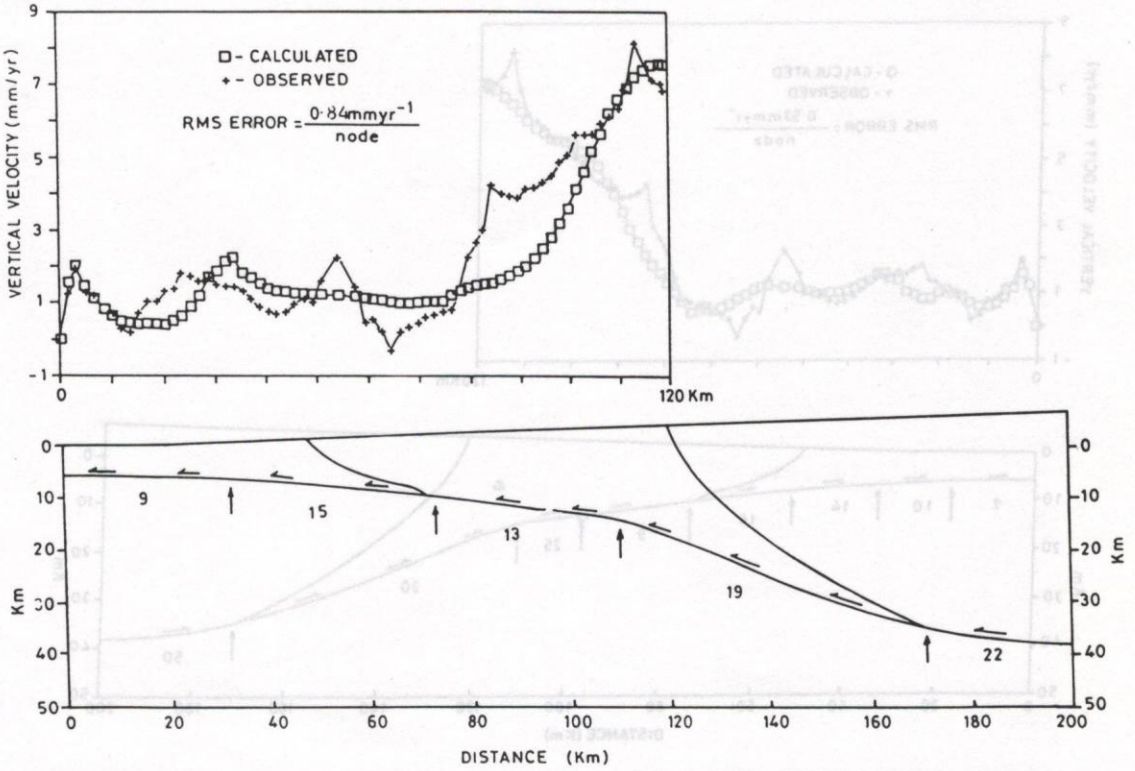

Fig. 8: The observed and the computed vertical velocities at the surface and the inverted slip rates (mm/yr) on different segments of the detachment.

low coupling also defines the part of the detachment on which small and moderate magnitude thrust earthquakes are proposed to occur. This correlation between earthquake activity and the slip rates on the detachment points to the presence of large strains on the high coupling segment on the detachment during the past.

Actually the interseismic uplift observed across the Nepal Himalaya are explained by two different models of subduction: (i) interseismic locking and aseismic creep occurring on the detachment respectively to the south and north of the Higher Himalaya, (ii) interseismic slip occurring on entire detachment. It has been well documented in literature that application of former model would imply accumulation of strains. Yet the results of the present analysis favours latter model. Thus our interest lies in identifying whether strains would be accumulating on the detachment if none of its portions is locked. In the next section we seek to answer this question.

STRAIN ACCUMULATION FOR EARTHQUAKES

We suggest that occurrence of interseismic thrust fault type slip (Chander and Gahalaut, 1994; Lisowski, et al., 1988; result of the present study), does not rule out the presence of accumulated strains instead it may even cause strains to accumulate. The following simple example of a book being dragged on a table highlights this situation.

Let a book be held upright on a table as shown in Fig. 12. When a horizontal force is applied on the book, first its pages bend in a fashion shown in Fig. 12 and then at a certain instant it starts sliding on the table. The book will continue to slide with a certain slip rate, maintaining its deformed shape (conditionally stable sliding)

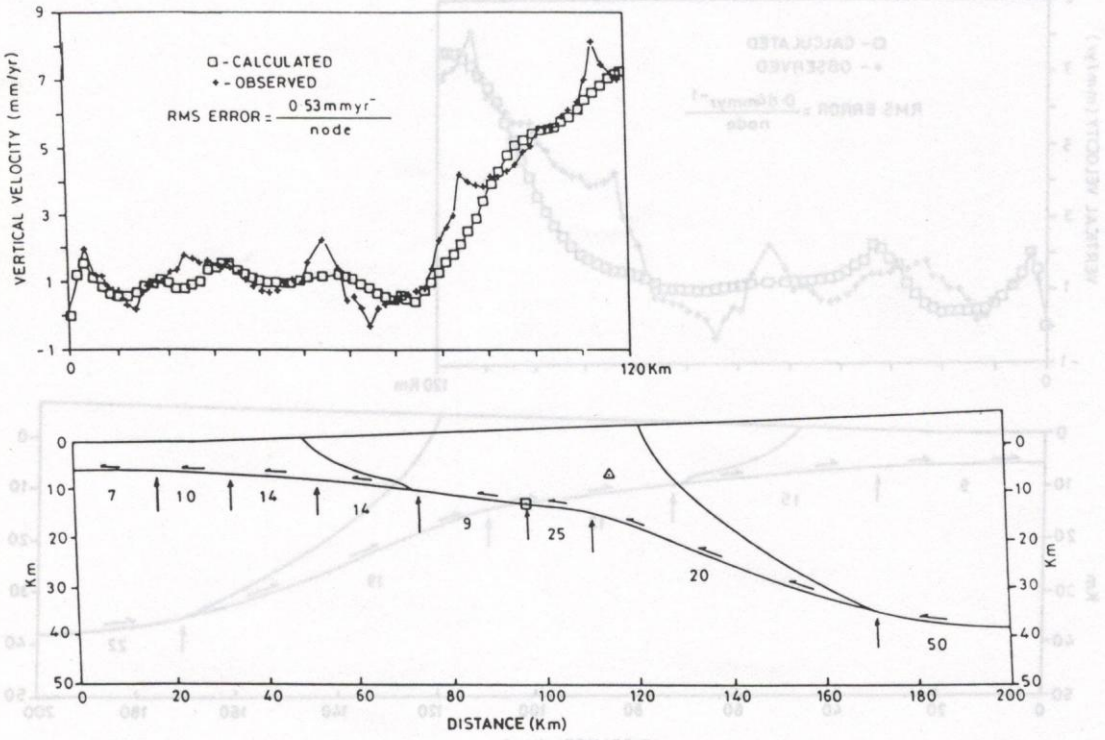

Fig. 9: The observed and the computed vertical velocities at the surface, the rms error between them and the inverted slip rates (mm/yr) on different segments representing the detachment in Nepal Himalaya. The high coupling sections with low updip slip rate than on adjoining segments is highlighted by dashed line.

provided its coupling with the table and force applied remain unchanged. A change in coupling would lead to a change (increase or decrease) in bending of the book. To understand the accumulation (or release) of strains close to the detachment, consider the situation shown in Fig. 13. Let 1, 2 and 3 represents three collinear points on the subducting plate, on the detachment and above the detachment respectively (Fig. 13). According to stick-slip motion models, points 1 and 2 are fully coupled during interseismic period and a downdip motion of subducting plate causes downdip displacement of point 2 relative to point 3 which represents accumulation of shear strains. In addition to this, a situation where point 2 is displaced updip relative to point 1, together with point 3 displaced even farther updip of point 2 also represent accumulation of shear strains in the overriding medium. This is what happens when we drag the book against the table. Thus, eventhough slip is occurring on the detachment, yet strains have been accumulated, represented as bending of the book, in the overlying medium. The physical justification to above kinematic description of the process of strain accumulation comes from the temporal variation in coupling on the detachment.

In case coupling increases with time, for example due to an increase in normal loads at the detachment (Pacheco et al., 1993), it will produce velocity strengthening effect through increasing the (rate dependent) friction and strain hardening (Cochard and Madariaga, 1996) thereby causing further shearing (bending) of the overriding medium due to decrease in updip slip rate of point 2 (Fig. 13). Similarly, a decrease in coupling would result in velocity weakening and reduction in shearing due to an increase in slip rate of point 2. So, from the above model, a decrease in updip slip rate is indicative of shear strain accumulation,

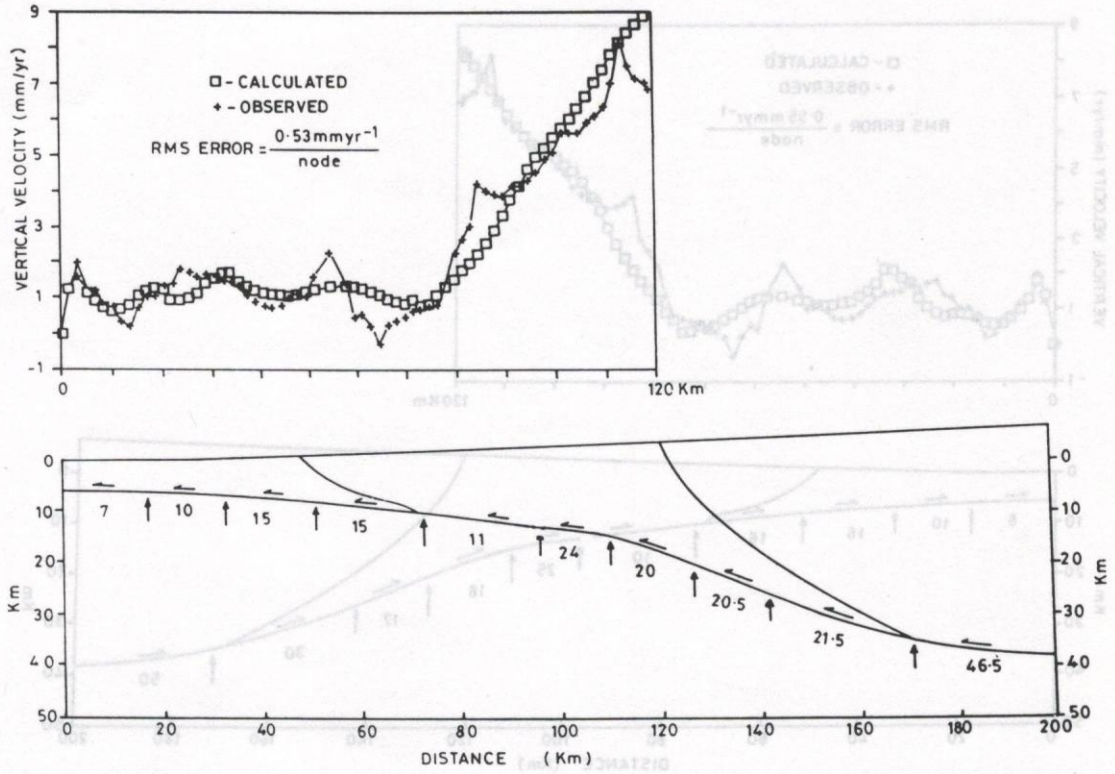

Fig. 10: The observed and the computed vertical velocities at the surface and the inverted slip rates (mm/yr) on different segments of the detachment.

and an increase in updip slip rate to release of accumulated shear strains at present times. In this context, the observed elevation changes in the Himalaya used for the analysis have been measured twice only, are not sufficient to infer about the changes in slip rates and hence the possible accumulation or release of shear strains on the detachment at present times. The above proposition of shear strain accumulation and release is supported by certain analyses suggesting a temporal variation in shear strain rate and coupling during earthquake cycles (Yoshioka, 1991; Bawden et al., 1997). The study by Bawden et al., (1997) measures horizontal shear strain rates for the preseismic, post seismic and recent periods near White Wolf fault, California. The results show low shearing rates during preseismic and recent periods while large ones during postseismic period. This indicate a general decrease in slip rate from post seismic to pre seismic times. The study by Yoshioka (1991) infers a temporal increase in coupling from interseismic to preseismic period along the Nankai trough. This is also in accordance with the proposed model in this paper where increase in coupling results in accumulation of shear strains through a decrease in slip rate which may culminate into occurrence of an earthquake.

Another proposition of strain accumulation with the occurrence of thrust fault type slip is also presented. The inferences based on geodetic and seismological observations suggest occurrence of non uniform slip during interseismic periods along the detachment (Pacheco et al., 1993; Savage, 1995; result of the present study). The large variation in slip on the fault during an earthquake has been associated, in addition to fixed geometrical/material properties, to the phenomenon of dynamically created barriers and the effect of velocity weakening (Cochard and Madariaga, 1996). Similarly, we propose that the segments of the Himalayan detachment with low interseismic slip rate may be acting as barriers to

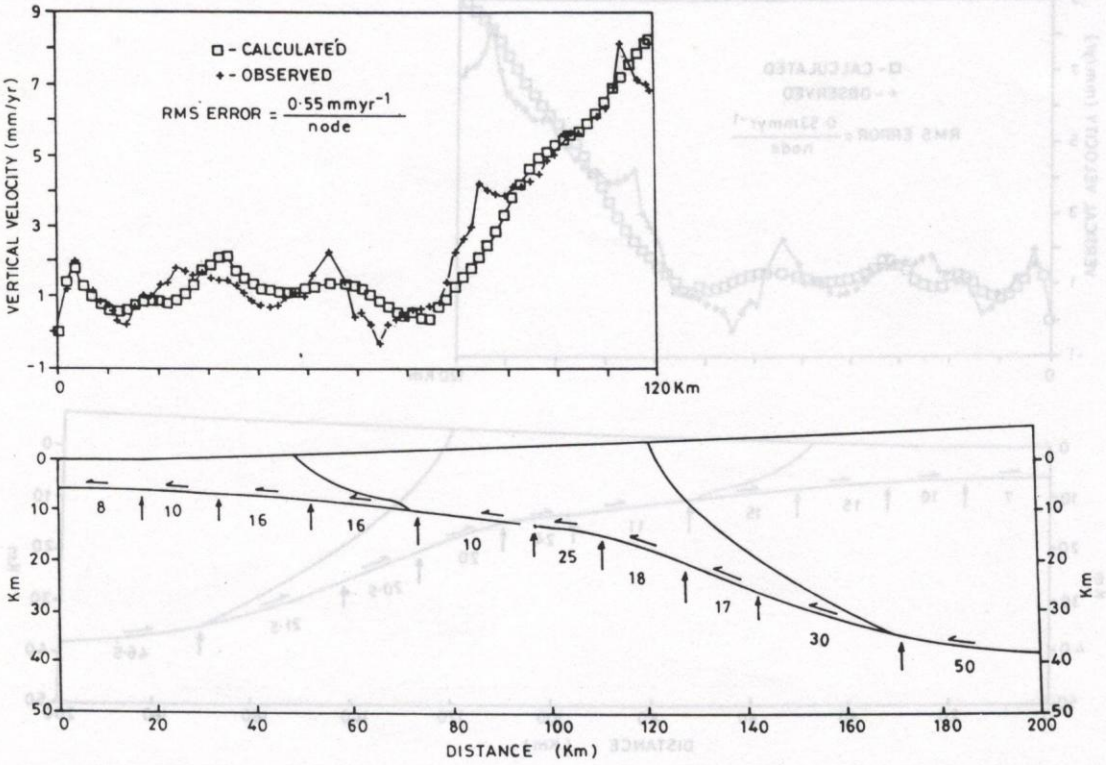

Fig. 11: The observed and the computed vertical velocities at the surface and the inverted slip rates (mm/yr) on different segments of the detachment for 173 element grid case.

the motion of adjacent northward segments with high slip rates. Hence, the difference in interseismic slip rates on the two adjacent segments of detachment with front segment (in updip direction) having lower slip rate than the rear one (in downdip direction), will be accumulated as compressive strains in continuum (mountain wedge interior). This model is different from the proposition of Savage (1995) in that none of the portion of the thrust zone is

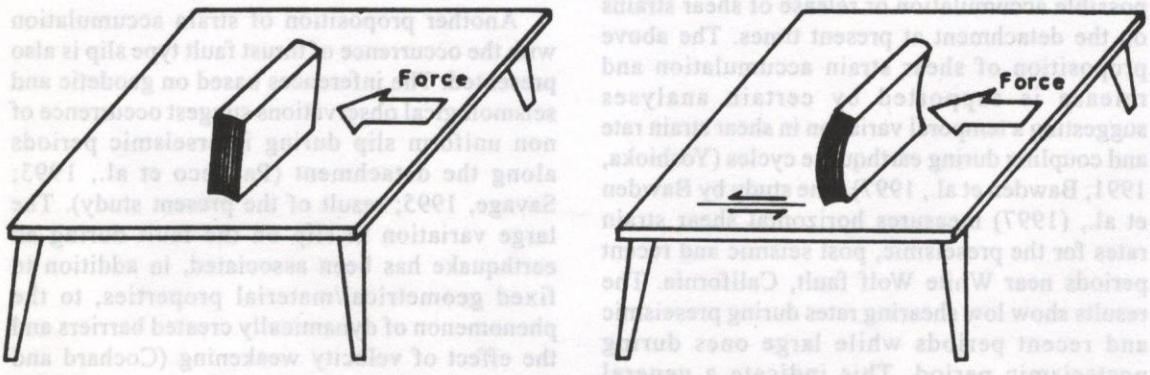

Fig. 12: When a horizontal force is applied to book held upright, its pages bend and it slides on the surface. A change in coupling between the book and the surface results in a change in this bending. This example highlights the process of strain accumulation, which can occur both before and after the initiation of sliding.

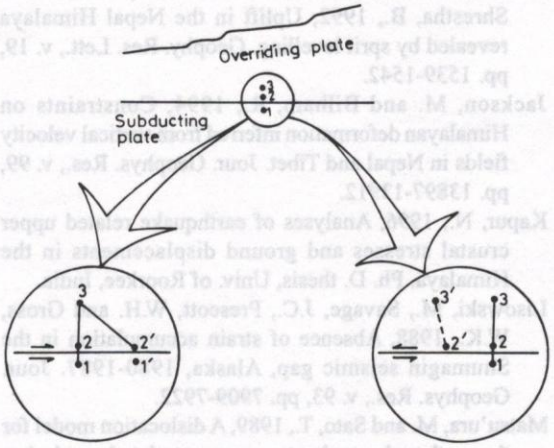

Fig. 13: Kinematics of the process of strain accumulation close to the detachment (a) in the presence of locking as expected from stick slip motion model (b) when locking is absent as proposed in this paper. Updip motion of point 3 relative to point 2 represents the accumulation of shear strains in both the situations.

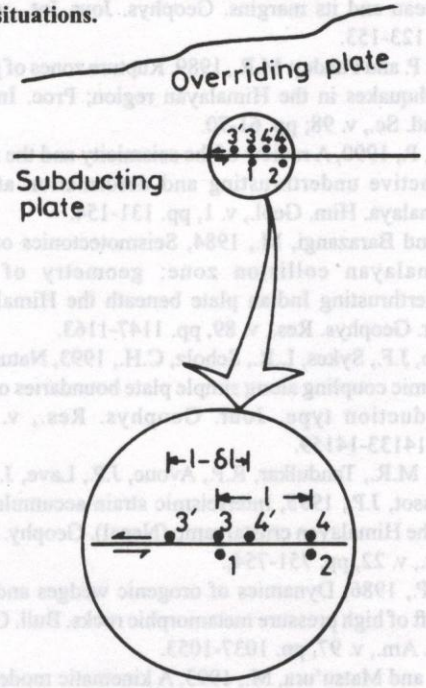

Fig. 14: Kinematics of compressive straining close to the detachment with simultaneous occurrence of thrust fault type slip along the detachment. Updip slip of point 3 and 4 resulting in a decrease in the distance between them represents compressive straining.

completely locked during interseismic periods and yet strains are accumulating.

To visualise above process of strain accumulation, consider the situation given in Fig. 14. According to stick slip motion models of the main thrust zone, points 1 and 2 of the subducting plate are fully coupled to points 3 and 4 of the overriding plate. A situation in which points 3 and 4 are displaced updip of points 1 and 2 respectively in such a manner so that the distance between points 3 and 4 is reduced, represents accumulation of strains due to compression.

From the above propositions it is suggested that even though shear strains on the Nepal Himalayan detachment may or may not be accumulating at present times yet strains due to compression would be accumulating on certain portions of the detachment. Thus, we can not rule out the possibility of strain accumulation even if thrust fault interseismic slip is taking place and no portion of the detachment is locked.

CONCLUSIONS

The analysis of the available interseismic elevation changes in the Nepal Himalaya for displacement rates on detachment infers the occurrence of thrust fault type slip, rather than normal fault type motion on it.

Occurrence of thrust fault type slip during interseismic period also suggest that the overriding and the subducting media may not be fully coupled as predicted by stick slip subduction models.

From the inferred interseismic slip rates on the detachment a section of high coupling (consisting of two nearly contiguous segments of low thrust fault type slip rate) bounded in front and rear by those of low coupling has been identified.

The proposed section of high coupling on detachment, having a length of 100 km coincides the inferred rupture zone of 1934 great Himalayan earthquake in the region. The portion of the detachment on which small and moderate magnitude thrust earthquakes are proposed to occur, also form a part of this section with high coupling.

In our view, occurrence of thrust fault type motion during interseismic period on the Himalayan detachment does not rule out the possibilities of the accumulation of shear as well as compressive strains for release in thrust earthquakes. Eventhough, the former strains may or may not be accumulating, yet the latter ones would be accumulating at present times on certain portions of the Nepal Himalayan detachment.

ACKNOWLEDGMENT

The suggestions by Dr. J.C. Savage of USGS helped to improve the quality of the paper.

REFERENCES

Armijo, R., Tapponier, P., Mercier, J.L. and Han, T., 1986, Quaternary extension in southern Tibet. Jour. Geophys. Res., v. 91, pp. 13803-13872.

Bawden, G.W., Donnellan, A., Kellogg, L.H., Dong, D. and Rundle, J.B., 1997, Geodetic measurements of horizontal strain near the White Wolf Fault, Kern County California, 1926–1923. Jour. Geophys. Res., pp. 4957-4967.

Bilham, R., Larson, K., Freymueller, J. and Project Idylhim members, 1997, GPS measurements of present day convergence across the Nepal Himalaya. Nature, v. 386, pp. 61-64.

Chander, R., 1989, Southern limits of major earthquakes ruptures along the Himalaya between longitudes 75° and 90° E. Tectonophysics, v. 170, pp. 115-123.

Chander, R. and Gahalaut, V.K., 1994, Preparation for great earthquakes seen in levelling observations along two lines across the Outer Himalaya. Curr. Sc., v. 67, pp. 531-534.

Cochard, A. and Madariaga, R., 1996, Complexity of seismicity due to highly rate-dependent friction, Jour. Geophys. Res., v. 101, pp. 25321-25336.

Dahlen, F. A. and Barr, T.D., 1989, Brittle frictional mountain building deformation and mechanical energy buget. Jour. Geophys. Res., v. 94, pp. 3906-3922.

Du, Y., Segall, P. and Gao, H., 1994, Dislocations in inhomogeneous media via a moduli perturbation approach: general formulation and two dimensional solutions. Jour. Geophys. Res., v. 99, pp. 13767-13779.

Hyndman, R.D. and Wang, K., 1993, Thermal constraints on the zone of major thrust earthquake failure: the cascadian subduction zone. Jour. Geophys. Res., v. 98, pp. 2039-2060.

Jackson, M., Barrientos, S., Bilham, R., Kayestha, D. and Shrestha, B., 1992, Uplift in the Nepal Himalaya revealed by sprit levelling. Geophy. Res. Lett., v. 19, pp. 1539-1542.

Jackson, M. and Bilham, R., 1994, Constraints on Himalayan deformation inferred from vertical velocity fields in Nepal and Tibet. Jour. Geophys. Res., v. 99, pp. 13897-13912.

Kapur, N., 1996, Analyses of earthquake related upper crustal stresses and ground displacements in the Himalaya. Ph. D. thesis, Univ. of Roorkee, India.

Lisowski, M., Savage, J.C., Prescott, W.H. and Gross, W.K., 1988, Absence of strain accumulation in the Shumagin seismic gap, Alaska, 1980-1987. Jour. Geophys. Res., v. 93, pp. 7909-7922.

Matsu'ura, M. and Sato, T., 1989, A dislocation model for the earthquake cycle at convergent plate boundaries. Geophys. J. Int., v. 96, pp. 23-32.

Meertens, C.M. and Wahr, J.M., 1986, Topographic effect on tilt, strain, and displacement measurements. Jour. Geoplys. Res., v. 91, pp. 14057-14062.

Molnar, P. and Lyon-Caen, H., 1989, Fault plane solutions of earthquakes and active tectonics of the Tibetan plateau and its margins. Geophys. Jour. Int., v. 99, pp. 123-153.

Molnar. P. and Pandey, M.R., 1989, Rupture zones of great earthquakes in the Himalayan region; Proc. Indian Acad. Sc., v. 98; pp. 61-70.

Molnar, P., 1990, A review of the seismicity and the rates of active underthrusting and deformation at the Himalaya. Him. Geol., v. 1, pp. 131-154.

Ni, J. and Barazangi, M., 1984, Seismotectonics of the Himalayan collision zone: geometry of the underthrusting Indian plate beneath the Himalaya. Jour. Geophys. Res., v. 89, pp. 1147-1163.

Pacheco, J.F., Sykes, L.R., Scholz, C.H., 1993, Nature of seismic coupling along simple plate boundaries of the subduction type. Jour. Geophys. Res., v. 98, pp. 14133-14159.

Pandey, M.R., Tandulkar, R.P., Avouc, J.P., Lave, J. and Massot, J.P., 1995, Interseismic strain accumulation on the Himalayan crustal ramp (Nepal). Geophy. Res. Lett., v. 22, pp. 751-754,.

Platt, J.P., 1986; Dynamics of orogenic wedges and the uplift of high pressure metamorphic rocks. Bull. Geol. Soc. Am., v. 97, pp. 1037-1053.

Sato, T. and Matsu'ura, M., 1993, A kinematic model for evolution of island arc-trench systems. Geophys. J. Int., v. 114, pp. 512-530.

Savage, J.C., 1995, Interseismic uplift at the Nankai subduction zone, south-west Japan, 1951-1990. Jour. Geophys. Res., v. 100, pp. 6339-6350.

Savage, J.C., 1983, A dislocation model of strain accumulation and release at a subduction zone. Jour. Geophys. Res., v. 88, pp. 4984-4996.

Savage, J.C., 1987, Effect of crustal layering upon dislocation modelling. Jour. Geophys. Res., v. 92, pp. 10595-10600.

Seeber, L. and Arnbruster, J.G., 1981, Great detachment earthquakes along the Himalayan arc and long term forcasting. In: D.W. Simpson and P.G. Richards (eds.), Earthquake Prediction, An international Review, Am. Geophys. Union, Mauric Ewing Ser., v. 4, pp. 259-279.

Shimazaki, K., 1974, Pre-seismic crustal deformation caused by an underthrusting oceanic plate, in eastern Hokkaido, Japan. Phys. Earth Planet. Inter., v. 8, pp. 148-157.

Singh, R.P., Li, Q. and Nyland, E., 1991, Lithospheric deformation beneath the Himalayan region. Phys. Earth Planet. Inter., v. 61, pp. 291-296.

Thatcher, W., 1984, The earthquake deformation cycle at the Nankai trough, southwest Japan. Jour. Geophys. Res., v. 89, pp. 3087-3101.

Thatcher, W. and Rundle, J.B., 1984, A viscoelastic coupling model for cyclic deformation due to periodically repeated earthquakes at subduction zones. Jour. Geophys. Res., v. 89, pp. 3087-3101.

Yin, A., 1993, Mechanics of wedge shaped fault blocks an elastic solution for compressional wedge. Jour. Geophys. Res., v. 98, pp. 14245-14256.

Yoshioka, S., 1991, The interplate coupling and stress accumulation process of large earthquakes along the Nankai trough, southwest Japan, derived from geodetic and seismic data. Phy. Earth and Planet. Int., v. 66, pp. 214-243.

Yoshioka, S., Yabuki, T., Sagiya, T., Taba, T. and Matsukra, M., 1993, Interplate coupling and relative plate motion in the Tokai district, central Japan, deduced from geodetic data inversion using ABIC. Geophys. J. Int., v. 113, pp. 607-621.